# Characterization of a Cyanobacterial Chloride-Pumping Rhodopsin and Its Conversion into a Proton Pump

**Takatoshi Hasemi, Takashi Kikukawa, Naoki Kamo, and Makoto Demura**

From the Faculty of Advanced Life Science, Hokkaido University, Sapporo 060-0810, Japan

Running title: Conversion of $Cl^-$-pumping rhodopsin into a $H^+$ pump

To whom correspondence should be addressed: Dr. Takashi Kikukawa, Faculty of Advanced Life Science, Hokkaido University, N10W8, Kita-ku, Sapporo 060-0810, Japan, Telephone: +81-11-706-3435; FAX: +81-11-706-2771; E-mail: kikukawa@sci.hokudai.ac.jp

**Keywords:** bioenergetics, membrane protein, photobiology, photoreceptor, proton pump, microbial rhodopsin, retinal proteins

**ABSTRACT:**
Light-driven ion-pumping rhodopsins are widely distributed in microorganisms and are now classified into the categories of outward $H^+$ and $Na^+$ pumps and an inward $Cl^-$ pump. These different types share a common protein architecture and utilize the photoisomerization of the same chromophore, retinal, to evoke photoreactions. Despite these similarities, successful pump-to-pump conversion had been confined to only the $H^+$ pump bacteriorhodopsin, which was converted to a $Cl^-$ pump in 1995 by a single amino acid replacement. In this study, we report the first success of the reverse conversion, from a $Cl^-$ pump to a $H^+$ pump. A novel microbial rhodopsin (MrHR) from the cyanobacterium *Mastigocladopsis repens* functions as a $Cl^-$ pump and belongs to a cluster that is far distant from the known $Cl^-$ pumps. With a single amino acid replacement, MrHR is converted to a $H^+$ pump in which dissociable residues function almost completely in the $H^+$ relay reactions. MrHR most likely evolved from a $H^+$ pump, but it has not yet been highly optimized into a mature $Cl^-$ pump.

Rhodopsins are ubiquitous membrane proteins that enable the cellular utilization of light as an information and energy source. According to their conserved residues, they are classified into two groups (1,2). One is animal rhodopsin, represented by visual pigments in the eyes. The other is microbial rhodopsin, which shows divergent functions in unicellular microorganisms, such as light-driven ion pumps and light sensors for phototaxis and the regulation of gene expression. Different from animal rhodopsins, the microbial sensors represent a minority of the microbial rhodopsins. However, microbial sensors have individualities in their signal-transduction modes, which include interactions with other membrane proteins, interactions with cytoplasmic components, and light-gated ion channel activity.

Microbial rhodopsins were originally discovered in highly halophilic archaea in the early 1970's – 1980's (3). Since 1999, their homologues have begun to be identified in various microorganisms inhabiting a broad range of environments (4-6). It is now clear that in the microbial world, ion-pumping rhodopsins are abundant and widely distributed. In microorganisms, these ion pumps are probably the most convenient system for light energy utilization. The first and second ion pumps to be discovered were bacteriorhodopsin (BR) (7) and halorhodopsin (HR) (8) from halophilic archaea, which are an outward $H^+$ pump and an inward $Cl^-$ pump, respectively. In 2000, an outward $H^+$ pump named proteorhodopsin (PR) was discovered in a marine proteobacterium (9). Later, the PR homologues were identified in eubacteria living in the oceans worldwide (10). Recently, two

groups of ion pumps, the outward $Na^+$ pump (NaR) and inward $Cl^-$ pump (ClR), were also discovered in eubacteria (11,12). Their representatives are *Krokinobacter eikastus* rhodopsin 2 (KR2) (13) and *Fulvimarina pelagi* rhodopsin (FR) (14), respectively. The phylogenetic position of these ion pumps is shown in Fig 1A. In contrast to their functional diversity, these ion pumps have essentially the same structural folds composed of seven helices and the chromophore retinal, which binds to a conserved lysine residue *via* a protonated Schiff base (PSB; deprotonated Schiff base is abbreviated as SB). In the dark, most ion-pumping rhodopsins dominantly contain retinal with the all-*trans* configuration, while some minorities such as BR and HR from archaeon *Halobacterium salinarum* (HsHR) can also accommodate 13-*cis* retinal (2). Regardless of this difference in the dark states, only the photoisomerization from all-*trans* to 13-*cis* can trigger the conformational changes for respective ion pumping functions. Thus, ion-pumping rhodopsins appear to share a common transport machinery, where the transportable ions are probably determined by essential residues at appropriate positions. This scenario was partially demonstrated in 1995, when the $H^+$ pump BR was converted to an inward $Cl^-$ pump by the single amino acid replacement of Asp85 with Thr, the corresponding amino acid in HR (15). However, the success of pump-to-pump conversion was confined to this BR case. The reverse conversion, that is, from a $Cl^-$ pump to a $H^+$ pump, has not been achieved (16-18) even after ten mutations of HR (18). Here, we report a new class composed of an inward $Cl^-$ pump and its conversion to an outward $H^+$ pump. Functional characterization was performed with a microbial rhodopsin from the cyanobacterium *Mastigocladopsis repens*, which was isolated from soil at Punta de la Mora, Tarragona in Spain. This microbial rhodopsin is designated as *M. repens* HR (MrHR) due to its similarities with HR. By a single amino acid replacement, MrHR begins to pump $H^+$ outwardly. Thus, this is the first successful conversion from an inward $Cl^-$ pump to an outward $H^+$ pump.

## EXPERIMENTAL PROCEDURES

*Phylogenetic Analysis*—The 57 amino acid sequences were aligned using MUSCLE. All sequence data were obtained from the NCBI database. The phylogenetic tree was constructed by using the maximum likelihood method, with bootstrap percentages based on 1,000 replications. Initial trees for the heuristic search were obtained by applying the neighbor-joining method (19). Evolutionary distances were calculated with the JTT matrix-based method (20). The branch lengths denote the number of amino acid substitutions. All analyses were performed using MEGA6.

*Gene preparation, protein expression and purification—Escherichia coli* strain DH5α was used for DNA manipulation. An MrHR gene (NCBI accession ID: WP_017314391) with codons optimized for *E. coli* expression was chemically synthesized (Funakoshi, Japan) and inserted into the NdeI/XhoI site of the pET-21c(+) vector (Merck Japan, Tokyo, Japan). This plasmid results in MrHR with additional amino acids in the C-terminus (-LEHHHHHH). The T74D mutation was introduced using the QuikChange Site-Directed Mutagenesis Kit (Stratagene, La Jolla, CA). The DNA sequences were confirmed by a standard method using an automated DNA sequencer (model 3100, Applied Biosystems, Foster City, CA). MrHR and the T74D mutant were expressed and purified from *E. coli* BL21(DE3) cells. The procedures were essentially the same as those previously described (21). The cells were grown at 37 ºC in 2×YT medium supplemented with 50 μg/mL ampicillin. At the late exponential growth phase, the expression was induced by the addition of 1 mM isopropyl-β-D-thiogalactpyranoside in the presence of 10 μM all-*trans* retinal. After 3 h of induction, pink-colored cells were harvested by centrifugation (6400 × g, 8 min at 4 °C) and washed once with buffer (50 mM Tris-HCl, pH 8.0) containing 5 mM $MgCl_2$. Then, the cells were broken with a French press (Ohtake, Tokyo, Japan) (100 MPa × 4 times). After removing the undisrupted cells by centrifugation (5600 × g, 10 min at 4 °C), the supernatant was ultracentrifuged (178,000 × g, 90 min at 4 °C). The collected cell membrane fraction was suspended with the same

buffer containing 300 mM NaCl and 5 mM imidazole and was then solubilized with 1.5% n-dodecyl β-D-maltopyranoside (DDM) (Dojindo Lab, Kumamoto, Japan) at 4 °C overnight. After removal of the insoluble fraction by ultracentrifugation (178,000 × g, 60 min at 4 °C), the solubilized MrHR proteins were subjected to Ni-NTA agarose (Qiagen, Hilden, Germany). The unbound proteins were removed by washing the column with 10 column volumes of wash buffer (50 mM sodium phosphate, pH 7.5) containing 400 mM NaCl, 50 mM imidazole and 0.05% DDM. The bound protein was eluted with buffer (50 mM Tris-HCl, pH 7.0) containing 300 mM NaCl, 500 mM imidazole and 0.1% DDM. The yield of MrHR was 15 mg from 1 L culture. The concentration was determined from the absorbance at 537 nm under an assumed extinction coefficient of 40,000 $M^{-1}cm^{-1}$. The purified samples were replaced with an appropriate buffer solution by passage over Sephadex G-25 in a PD-10 column (Amersham Bioscience, Uppsala, Sweden).

*Ion-pump activity measurements*—The MrHR activity was measured in *E. coli* suspensions using a conventional pH electrode method (22), which detects the pH changes by the pump activity of $H^+$ itself or passive $H^+$ transfer in response to the membrane potential created by the pump activity for another ion. The *E. coli* suspensions were prepared as follows. The cells expressing MrHR were harvested at 3,600 g for 5 min at 4 ºC and washed twice with an unbuffered solution containing 200 mM salt (NaCl, Choline-Cl, NaBr, NaI or $NaNO_3$). They were resuspended in the same salt solution and gently shaken overnight at 4 ºC in the presence of 10 μM carbonyl cyanide m-chlorophenylhydrazone (CCCP). Then, the cells were washed twice with the same salt solution without CCCP and finally suspended at an $A_{660}$ of 0.5. This cell density was approximately 5% of the corresponding value for the original culture medium. As deduced from the purification yield, the original culture medium contains at least 15 μg/mL MrHR. Thus, the cell suspensions for the activity measurements contain at least 0.75 μg/mL of MrHR. For the activation of MrHR, 530 ± 17.5 nm green LED (LXHL-LM5C, Philips Lumileds Lighting Co., San Jose, CA) was used.

*HPLC analysis*—The retinal configurations of MrHR were examined in both of the dark/light-adapted states. For dark adaptation, the MrHR samples were kept in the dark for 1 week in 10 mM MOPS, pH 6.5, containing 100 mM NaCl and 0.05% DDM. For light adaptation, the samples were irradiated for 2 min by green LED light as described above. MrHR undergoes a prolonged photocycle as described below. To avoid the contamination of retinal in the photolyzed state, the retinal oxime extraction was carried out after 1 min incubation in the dark. The extraction and the following HPLC analysis was performed as previously described (22).

*Absorption spectra measurements and Flash photolysis*—UV-visible spectra of MrHR samples were measured with a UV-1800 spectrometer (Shimadzu, Kyoto, Japan). Flash-induced absorbance changes were obtained in the 5 μs to 10 s time range on a single wavelength kinetic system. For the photoexcitation, the second harmonic (7 ns, 532 nm) of a Q-switched Nd:YAG laser (Surelite I-10, Continuum, Santa Clara, CA) was used. The details have been previously described (21). To improve the S/N ratio, 30 laser pulses were used at each measurement wavelength. All measurements were performed at 25 ºC.

## RESULTS AND DISCUSSION

*Mastigocladopsis repens*, isolated from the surface of soft powdery calcareous soil, is a blue-green alga belonging to the cyanobacterial order Stigonematales and was morphologically characterized according to the filaments it forms, which have many branches (23). In 2013, the existence of a gene encoding a microbial rhodopsin was revealed by whole genome sequencing of *M. repens* (24). We named this microbial rhodopsin "*M. repens* halorhodopsin (MrHR)" after its photochemical properties, described below. At present, six other homologues of MrHR are found in the NCBI database. Figure 1A shows the phylogenetic tree of microbial rhodopsins, which revealed that

MrHR homologues constitute a new clade that is distinct from the known microbial rhodopsins. The six homologues are also encoded in cyanobacteria and share 63-89% amino acid identities with MrHR. Meanwhile, the host strains belong to different cyanobacterial orders (Chroococcales and Nostocales) from *M. repens*, reflecting morphological differences. The phylogenetic relationships of MrHR homologues are shown in Fig 1B together with the names, orders and sources of their host strains. In addition to *M. repens*, all other genomes were sequenced (24-28). Cyanobacteria are a genetically diverse group and are widespread in fresh water, marine, terrestrial and extreme environments such as hot springs and salt lakes. However, out of the seven strains of MrHR homologues, six were isolated from terrestrial environments, such as soil and rock scrapings, and biofilms on stone monuments and building facades (Fig 1B) (23,29,30). Correspondingly, the desiccation resistance was experimentally confirmed for several strains (31). Two strains also contain the gene for *Anabaena* sensory rhodopsin (ASR), a putative sensor for chromatic adaptation that was originally discovered in the cyanobacterium *Anabaena* sp. PCC7120 (32). The other five strains do not contain other microbial rhodopsin genes.

Microbial rhodopsins are largely categorized into ion pumps and sensors. All ion pumps are solely encoded in their respective operons in the genomes, whereas all sensors are encoded to be adjacent to the genes encoding the cognate transducers within the same operons. For MrHR homologues, their genes are solely encoded, implying that they function as ion pumps. Previous studies on ion pumps (12,13) have indicated that three amino acids are responsible for determining the transportable ions (Fig 2A and B). For $H^+$ pumps, a $H^+$ from PSB is translocated during the photoreaction. This $H^+$ is initially transferred to D85 in BR (D97 in PR), and SB subsequently accepts a $H^+$ from D96 in BR (E108 in PR) (Fig 2A). These residues are often referred to as the $H^+$ acceptor and donor, respectively. For $Cl^-$ pumps, the acceptor is replaced with a 'T' in HR and 'N' in FR (Fig 2B), which enables the binding of substrate $Cl^-$ as the counter ion of the PSB. Furthermore, for HR and KR2, another residue corresponding to T89 in BR is known to play a crucial role (13,21): These residues are 'S' in HR and 'D' in KR2, respectively (Fig 2B). Thus, three residues (D85, T89, and D96 in BR) are now designated as the "motif": These are DTD and DTE for BR and PR, TSA for HR, and NTQ and NDQ for FR and KR2 (Fig 2B). For MrHR, the motif is TSD (Fig 2A and B), which is close to TSA in HR. This implies that MrHR may pump $Cl^-$ inwardly, despite a low amino acid identity of 22% for HR and 12% for FR. The identities for the $H^+$ pumps are also low: 29% for BR and 17% for PR. However, the donor in the $H^+$ pumps is conserved as 'D' in MrHR, similar to BR(D) or PR(E). Furthermore, MrHR conserves E194 and E204 in BR, which consists of the $H^+$ releasing complex to the extracellular medium (Fig 2B). Thus, MrHR conserves the residues that are characteristic of both the $Cl^-$ pump (HR) and the $H^+$ pump (BR and PR).

In this study, we expressed MrHR in the cell membrane of *Escherichia coli* and investigated the ion-pumping activity using the light-induced pH changes of the cell suspensions (Fig 3). In a NaCl solution, light-induced alkalization was observed. This pH change was not abolished by the addition of the protonophore CCCP, which eliminates the electrochemical gradient of the proton (33). This means that the alkalization was not caused by the active proton transport but was caused by the passive proton influx in response to the interior negative membrane potential, which should be created by outward $Na^+$ or inward $Cl^-$ translocation. In Choline-Cl, alkalization was also observed. Because choline is a large organic cation, microbial rhodopsin cannot transport it. This indicates that MrHR functions as a light-driven inward $Cl^-$ pump. The pump activity decreased in NaBr and disappeared in NaI and $NaNO_3$. Thus, MrHR does not pump $Na^+$ but does pump smaller anions. The transportable anions are severely restricted to only $Cl^-$ and $Br^-$, different from HR and FR, which can even transport $NO_3^-$ (14,33).

The retinal isomer composition of MrHR was examined by HPLC analysis (Fig. 4). As described above, BR and HsHR in the dark states

can accommodate both all-*trans* and 13-*cis* retinals and show so-called "light-dark adaptation" (2). In their light-adapted states after continuous illumination, the unphotolyzed states predominantly contain all-*trans* retinal. Upon dark adaptation, their 13-*cis* contents increase approximately 50%. For MrHR (Fig 4), the isomer composition does not depend upon the dark/light adaptation and is predominantly all-*trans*, similar to most ion-pumping rhodopsins. Thus, the all-*trans* retinal is responsible for the ion-pumping function of MrHR.

Anion binding near the PSB was monitored by the color change of retinal using purified MrHR (Fig 5A). For other $Cl^-$ pumps, $Cl^-$ binding causes a blueshift (14,34), except for HsHR (22). In contrast, a large redshift occurs for MrHR by its binding of $Cl^-$, suggesting the differences in the $Cl^-$ binding site from other $Cl^-$ pumps. Similar redshifts were also observed for $Br^-$ and even for $I^-$ and $NO_3^-$. The dissociation constants ($K_d$) were determined from the absorbance changes at 550 nm (Fig 5B), and the results are summarized in Table 1. The $K_d$ values are close to those of HR, except for $NO_3^-$ (171 mM): HR binds $NO_3^-$ more strongly ($K_d$ ~ 16 mM) (35), whereas FR binds these ions more weakly ($K_d$ = 40 – 130 mM) (14). These results indicate that MrHR can bind $I^-$ and $NO_3^-$ but cannot transport them. These larger ions may be impossible to move toward a cytoplasmic half channel over the PSB region. Compared with HR and FR, the ion translocation pathway might be narrow and act as an ion-selective filter.

We also characterized the photocycle of MrHR by a flash photolysis method. Time-dependent absorbance changes at selected wavelengths are shown in Fig 5C, which indicates that the photocycle of MrHR is very slow due to the prolonged decay of the last intermediate (540 nm). Ion-pumping rhodopsins transport one ion during a single turnover of photocycle and generally undergo fast photocycles (< 100 ms), which enable the generation of a large transmembrane electrochemical potential under constant illumination. On the other hand, similar to HR and FR, no absorbance change at 400 nm was observed throughout the photocycle (14,34,36), indicating that there was no formation of a M intermediate, which is expected in $H^+$ pumps and reflects the deprotonation of PSB. The observed intermediates and the order of their appearance resembles those of HR. These intermediates are (the estimated $\lambda_{max}$ are indicated in the parentheses): K (540 nm) → L (460 nm) → N (460 nm) + O (620 nm) → MrHR' (540 nm). "N (460 nm) + O (620 nm)" means that the quasi-equilibrium between N and O appeared in the time period between 3 – 50 ms. A similar equilibrium was also observed for HR (34,37). The last intermediate MrHR' corresponds to HR' in HR but has a substantially longer lifetime (~ 6 s).

The slow photocycle of MrHR might reflect some differences in the physiological role from other $Cl^-$-pumping rhodopsins. Although the details are not fully resolved, the $Cl^-$ pumps are believed to play roles in light-driven ATP production and/or maintaining the cellular osmotic balance during the volume increase of the growing cell (38-41). All host strains of MrHR homologues contain a photosynthetic apparatus. Thus, the slow photocycle of MrHR seems to contribute little to cellular ATP production under illumination. Instead, MrHR might relate to a regulation of osmotic pressure. Unlike aquatic cells harboring other $Cl^-$ pumps, most host strains of MrHR homologues inhabit terrestrial and non-aquatic environments, where the cells are occasionally exposed to drought stress. Thus, the cells might utilize MrHR homologues to survive in the non-aquatic habitats. Under desiccated conditions, the internal salt concentration should be increased to preserve the intracellular water content. Due to the interior negative membrane potential, cations could be passively transported inside. However, anions need an active transport system, such as MrHR. Thus, a simple scenario might be that MrHR elevates the intracellular osmotic pressure, which in turn preserves the intracellular water content under drought conditions. For further discussion, we must await future investigations.

MrHR conserves the $H^+$ donor residue in the $H^+$ pump, which is an essential residue in the $H^+$ pump. Thus, we attempted the conversion of

the MrHR to a $H^+$ pump; a mutant T74D was made in which the Asp residue was introduced as a possible proton acceptor. The $\lambda_{max}$ of T74D is located at 522 nm (Fig 6A) and did not change upon the addition of $Cl^-$. This indicates that there is no chloride binding near the PSB. The HPLC analyses showed that the retinal isomer composition is predominantly all-*trans* ( > 95%) in both dark and light-adapted states, similar to wild-type MrHR. Next, we examined the ion-pumping activity using the pH change of the *E. coli* suspension. The results are shown in Fig 6B, which indicates the opposite pH change to the wild-type MrHR. Even in the NaCl solution, light-induced acidification was observed, showing proton extrusion. This pH change was decreased by the addition of CCCP, indicating that T74D actively pumps protons outward. Thus, a successful conversion from a $Cl^-$ pump to a $H^+$ pump was effected by the single amino acid replacement. Corresponding to this conversion, T74D undergoes a totally different photocycle from that of wild-type MrHR (Fig 6C). Specifically, the M-formation (400 nm) was observed, indicating that the introduced Asp residue acts as a $H^+$ acceptor from PSB. For HR, a T-to-D mutation was never observed to induce M-formation (16-18). For natural $H^+$ pumps in the dark, SB is protonated while the acceptor is deprotonated because the SB has a larger pKa than the acceptor. M-formation requires the inversion of the pKa values: The pKa of the acceptor must become larger than that of SB. T74D accomplishes these pKa changes. Following M decay, two intermediates appear sequentially, corresponding to N (470 nm) and O (590 nm) in BR. For $H^+$ pumps, the donor facilitates both M-N and N-O transitions because the M-N transition reflects proton movement from the donor to SB, and the subsequent N-O transition reflects proton uptake from the cytoplasmic medium by the donor. Thus, the donor-lacking mutants of $H^+$ pumps undergo substantially slower transitions after M formation (42,43). Interestingly, both transitions in T74D are fast compared with natural $H^+$ pumps, indicating that the donor functions very well. Moreover, M, N and O appear sequentially without quasi-equilibrium. This reflects the strict "accessibility switch" of the donor, which communicates with SB during the M-N transition; then, the accessibility switches to the cytoplasmic medium to facilitate the N-O transition. In a $H^+$ pump, this switch contributes to the one-way (irreversible) $H^+$ transport (42,43). These facts indicate that T74D contains the structural factors as well as the essential residues for an effective $H^+$ pump.

The overall photocycle of T74D resembles that of natural $H^+$ pumps but is prolonged due to the last intermediate (520 nm), which resembles MrHR' in the wild-type photocycle. A similar intermediate was also observed in PR (44), but MrHR' in T74D has a substantially long lifetime (~3 s). Another difference from a natural $H^+$ pump is the formation of an unknown intermediate (hereafter called X) at approximately 440 nm. X is formed almost simultaneously with the M-decay, but it decays independently of N and O. Thus, X probably forms from M by a branching process. SB reprotonates during the M-decay. For the M-N transition, the donor provides this proton. For the M-X transition, the proton is probably provided through another pathway, implying no contribution of X to the $H^+$ pumping activity. In natural $H^+$ pumps, the antecedent deprotonation of SB triggers the accessibility switching of SB from the acceptor to donor, which enables the exclusive $H^+$ transfer from the donor to SB (42,43). In T74D, this switching might not be stringently controlled.

MrHR functions as an inward $Cl^-$ pump but undergoes a prolonged photocycle. The donor residue is not essential for $Cl^-$-pumping activity, which was confirmed by the alanine replacement mutant (data not shown). In contrast, in T74D, both the introduced acceptor and the conserved donor function are comparable with those in natural $H^+$ pumps, which suggests that MrHR evolved from a $H^+$ pump, but the residues and the structure have not been optimized into a mature $Cl^-$ pump. The mutant T74D has reduced $H^+$ pumping activity as compared to natural $H^+$ pumps because of the slow decay of the last intermediate and the formation of the X intermediate. These weaknesses are probably related to the lost mechanisms, which are

important for a $H^+$ pump but not for a $Cl^-$ pump. Thus, comparable studies of MrHR, $Cl^-$ pumps and $H^+$ pumps might provide insight into how sophisticated $Cl^-$ pumps evolved from $H^+$ pumps.

**Conflict of interest:** The authors declare that they have no conflicts of interest with the contents of this article.

**Authors contributions:** T. H. performed all experiments and wrote the paper. T. K. designed the study and wrote most of the paper. N. K. and M. D. provided technical assistance and contributed to the preparation of the manuscript. All authors reviewed the results and approved the final version of the manuscript.

## REFERENCES


1. Heberle, J., Deupi, X., and Schertler, G. (2014) Retinal proteins - you can teach an old dog new tricks. *Biochim. Biophys. Acta* **1837**, 531-532
2. Ernst, O. P., Lodowski, D. T., Elstner, M., Hegemann, P., Brown, L. S., and Kandori, H. (2014) Microbial and animal rhodopsins: structures, functions, and molecular mechanisms. *Chem. Rev.* **114**, 126-163
3. Grote, M., and O'Malley, M. A. (2011) Enlightening the life sciences: the history of halobacterial and microbial rhodopsin research. *FEMS Microbiol. Rev.* **35**, 1082-1099
4. Bieszke, J. A., Braun, E. L., Bean, L. E., Kang, S., Natvig, D. O., and Borkovich, K. A. (1999) The *nop-1* gene of *Neurospora crassa* encodes a seven transmembrane helix retinal-binding protein homologous to archaeal rhodopsins. *Proc. Natl. Acad. Sci. U.S.A.* **96**, 8034
5. Spudich, J. L., and Jung, K.-H. (2005) Microbial rhodopsin: Phylogenetic and functional diversity. in *Handbook of photosensory receptors* (Briggs, W. R., and Spudich, J. L. eds.), Wiley-VCH Verlag, Weinheim. pp 1-23
6. Inoue, K., Kato, Y., and Kandori, H. (2014) Light-driven ion-translocating rhodopsins in marine bacteria. *Trends. Microbiol.* **23**, 91-98
7. Oesterhelt, D., and Stoeckenius, W. (1971) Rhodopsin-like protein from the purple membrane of *Halobacterium halobium*. *Nature* **233**, 149-152
8. Matsuno-Yagi, A., and Mukohata, Y. (1977) Two possible roles of bacteriorhodopsin; a comparative study of strains of *Halobacterium halobium* differing in pigmentation. *Biochem. Biophys. Res. Commun.* **78**, 237-243
9. Béjà, O., Aravind, L., Koonin, E. V., Suzuki, M. T., Hadd, A., Nguyen, L. P., Jovanovich, S. B., Gates, C. M., Feldman, R. A., Spudich, J. L., Spudich, E. N., and DeLong, E. F. (2000) Bacterial Rhodopsin: Evidence for a New Type of Phototrophy in the Sea. *Science* **289**, 1902-1906
10. Béjà, O., Pinhassi, J., and Spudich, J. L. (2013) Proteorhodopsins: widespread microbial light-driven proton pumps. in *Encyclopedia of Biodiversity* (Levin, S. A. ed.), 2nd Ed., Elsevier, New York. pp 280-285
11. Jung, K. H. (2012) New type of cation pumping microbial rhodopsins in marine bacteria. in *244th ACS National Meeting & Exposition*, Philadelphia, PA
12. Yoshizawa, S., Kumagai, Y., Kim, H., Ogura, Y., Hayashi, T., Iwasaki, W., DeLong, E. F., and Kogure, K. (2014) Functional characterization of flavobacteria rhodopsins reveals a unique class of light-driven chloride pump in bacteria. *Proc. Natl. Acad. Sci. U.S.A.* **111**, 6732-6737

13. Inoue, K., Ono, H., Abe-Yoshizumi, R., Yoshizawa, S., Ito, H., Kogure, K., and Kandori, H. (2013) A light-driven sodium ion pump in marine bacteria. *Nat. Commun.* **4**, 1678
14. Inoue, K., Koua, F. H., Kato, Y., Abe-Yoshizumi, R., and Kandori, H. (2014) Spectroscopic study of a light-driven chloride ion pump from marine bacteria. *J. Phys. Chem. B* **118**, 11190-11199
15. Sasaki, J., Brown, L. S., Chon, Y. S., Kandori, H., Maeda, A., Needleman, R., and Lanyi, J. K. (1995) Conversion of bacteriorhodopsin into a chloride ion pump. *Science* **269**, 73-75
16. Havelka, W. A., Henderson, R., and Oesterhelt, D. (1995) Three-dimensional structure of halorhodopsin at 7 A resolution. *J. Mol. Biol.* **247**, 726-738
17. Váró, G., Brown, L. S., Needleman, R., and Lanyi, J. K. (1996) Proton transport by halorhodopsin. *Biochemistry* **35**, 6604-6611
18. Muroda, K., Nakashima, K., Shibata, M., Demura, M., and Kandori, H. (2012) Protein-bound water as the determinant of asymmetric functional conversion between light-driven proton and chloride pumps. *Biochemistry* **51**, 4677-4684
19. Saitou, N., and Nei, M. (1987) The neighbor-joining method: a new method for reconstructing phylogenetic trees. *Mol. Biol. Evol.* **4**, 406-425
20. Jones, D. T., Taylor, W. R., and Thornton, J. M. (1992) The rapid generation of mutation data matrices from protein sequences. *Comput. Appl. Biosci.* **8**, 275-282
21. Sato, M., Kikukawa, T., Araiso, T., Okita, H., Shimono, K., Kamo, N., Demura, M., and Nitta, K. (2003) Roles of Ser130 and Thr126 in chloride binding and photocycle of *pharaonis* halorhodopsin. *J. Biochem.* **134**, 151-158
22. Yamashita, Y., Kikukawa, T., Tsukamoto, T., Kamiya, M., Aizawa, T., Kawano, K., Miyauchi, S., Kamo, N., and Demura, M. (2011) Expression of *salinarum* halorhodopsin in *Escherichia coli* cells: solubilization in the presence of retinal yields the natural state. *Biochim. Biophys. Acta* **1808**, 2905-2912
23. Hernández-Mariné, M., Fernández, M., and Merino, V. (1992) *Mastigocladopsis repens* (Nostochopsaceae), a new cyanophyte from Spanish soils. *Cryptogamie, Algol.* **13**, 113-120
24. Shih, P. M., Wu, D., Latifi, A., Axen, S. D., Fewer, D. P., Talla, E., Calteau, A., Cai, F., Tandeau de Marsac, N., Rippka, R., Herdman, M., Sivonen, K., Coursin, T., Laurent, T., Goodwin, L., Nolan, M., Davenport, K. W., Han, C. S., Rubin, E. M., Eisen, J. A., Woyke, T., Gugger, M., and Kerfeld, C. A. (2013) Improving the coverage of the cyanobacterial phylum using diversity-driven genome sequencing. *Proc. Natl. Acad. Sci. U.S.A.* **110**, 1053-1058
25. Chandrababunaidu, M. M., Singh, D., Sen, D., Bhan, S., Das, S., Gupta, A., Adhikary, S. P., and Tripathy, S. (2015) Draft Genome Sequence of *Tolypothrix boutellei* Strain VB521301. *Genome Announc.* **3**, e00001-15
26. Singh, D., Chandrababunaidu, M. M., Panda, A., Sen, D., Bhattacharyya, S., Adhikary, S. P., and Tripathy, S. (2015) Draft Genome Sequence of Cyanobacterium *Hassallia byssoidea* Strain VB512170, Isolated from Monuments in India. *Genome Announc.* **3**, e00064-15
27. Das, A., Panda, A., Singh, D., Chandrababunaidu, M. M., Mishra, G. P., Bhan, S., Adhikary, S. P., and Tripathy, S. (2015) Deciphering the Genome Sequences of the Hydrophobic Cyanobacterium *Scytonema tolypothrichoides* VB-61278. *Genome Announc.* **3**, e00228-15
28. Das, S., Singh, D., Madduluri, M., Chandrababunaidu, M. M., Gupta, A., Adhikary, S. P., and Tripathy, S. (2015) Draft Genome Sequence of Bioactive-Compound-Producing Cyanobacterium *Tolypothrix campylonemoides* Strain VB511288. *Genome Announc.* **3**, e00226-15
29. Stanier, R. Y., Kunisawa, R., Mandel, M., and Cohen-Bazire, G. (1971) Purification and properties of unicellular blue-green algae (order *Chroococcales*). *Bacteriol. Rev.* **35**, 171-205
30. Rippka, R., Deruelles, J., Waterbury, J. B., Herdman, M., and Stanier, R. Y. (1979) Generic assignments, strain histories and properties of pure cultures of cyanobacteria. *J. Gen. microbiol.* **111**, 1-61

31. Keshari, N., and Adhikary, S. P. (2013) Characterization of cyanobacteria isolated from biofilms on stone monuments at Santiniketan, India. *Biofouling* **29**, 525-536
32. Jung, K.-H., Trivedi, V. D., and Spudich, J. L. (2003) Demonstration of a sensory rhodopsin in eubacteria. *Mol. Microbiol.* **47**, 1513-1522
33. Schobert, B., and Lanyi, J. K. (1982) Halorhodopsin is a light-driven chloride pump. *J. Biol. Chem.* **257**, 10306-10313
34. Váró, G., Brown, L. S., Sasaki, J., Kandori, H., Maeda, A., Needleman, R., and Lanyi, J. K. (1995) Light-driven chloride ion transport by halorhodopsin from *Natronobacterium pharaonis*. I. The photochemical cycle. *Biochemistry* **34**, 14490-14499
35. Scharf, B., and Engelhard, M. (1994) Blue halorhodopsin from *Natronobacterium pharaonis*: wavelength regulation by anions. *Biochemistry* **33**, 6387-6393
36. Váró, G., Zimányi, L., Fan, X., Sun, L., Needleman, R., and Lanyi, J. K. (1995) Photocycle of halorhodopsin from *Halobacterium salinarium*. *Biophys. J.* **68**, 2062-2072
37. Hasegawa, C., Kikukawa, T., Miyauchi, S., Seki, A., Sudo, Y., Kubo, M., Demura, M., and Kamo, N. (2007) Interaction of the halobacterial transducer to a halorhodopsin mutant engineered so as to bind the transducer: $Cl^-$ circulation within the extracellular channel. *Photochem. Photobiol.* **83**, 293-302
38. Oesterhelt, D. (1995) Structure and function of halorhodopsin. *Isr. J. Chem.* **35**, 475-494
39. Avetisyan, A. V., Kaulen, A. D., Skulachev, V. P., and Feniouk, B. A. (1998) Photophosphorylation in alkalophilic halobacterial cells containing halorhodopsin: chloride-ion cycle? *Biochemistry (Moscow)* **63**, 625-628
40. Ihara, K., Narusawa, A., Maruyama, K., Takeguchi, M., and Kouyama, T. (2008) A halorhodopsin-overproducing mutant isolated from an extremely haloalkaliphilic archaeon *Natronomonas pharaonis*. *FEBS Lett.* **582**, 2931-2936
41. Falb, M., Pfeiffer, F., Palm, P., Rodewald, K., Hickmann, V., Tittor, J., and Oesterhelt, D. (2005) Living with two extremes: conclusions from the genome sequence of *Natronomonas pharaonis*. *Genome Res.* **15**, 1336-1343
42. Balashov, S. P. (2000) Protonation reactions and their coupling in bacteriorhodopsin. *Biochim. Biophys. Acta* **1460**, 75-94
43. Lanyi, J. K. (2004) Bacteriorhodopsin. *Annu. Rev. Physiol.* **66**, 665-688
44. Váró, G., Brown, L. S., Lakatos, M., and Lanyi, J. K. (2003) Characterization of the photochemical reaction cycle of proteorhodopsin. *Biophys. J.* **84**, 1202-1207


**FOOTNOTES**

This work was supported by JSPS KAKENHI to T.K. (26440042).

The abbreviations used are: BR, bacteriorhodopsin; HR, halorhodopsin; PR, proteorhodopsin; NaR, $Na^+$-pumping rhodopsin; ClR, $Cl^-$-pumping rhodopsin; KR2, *Krokinobacter eikastus* rhodopsin 2; FR, *Fulvimarina pelagi* rhodopsin; NpHR, HR from *Natronomonas pharaonis*; HsHR, HR from *Halobacterium salinarum*; PSB, protonated Schiff base; SB, deprotonated Schiff base; MrHR, *Mastigocladopsis repens* HR; DDM, n-dodecyl β-D-maltopyranoside; CCCP, carbonyl cyanide m-chlorophenylhydrazone; ASR, *Anabaena* sensory rhodopsin; $K_d$, dissociation constant.

**FIGURE LEGENDS**

**FIGURE 1.** Phylogenetic relationships of microbial rhodopsins. (*A*) Unrooted tree of microbial rhodopsins showing their functional diversity. The representative ion pumps are shown with the circles. Green is the clade consisting of the MrHR homologues. (*B*) Phylogenetic tree of the MrHR homologues. Their NCBI accession IDs are indicated in the parentheses. The strains labeled with closed circles also contain the ASR gene. Other symbols indicate the cyanobacterial orders and the sources of the host strains. In both trees, nodes with less than 50% bootstrap percentages are collapsed.

**FIGURE 2.** (*A*) Positions of three amino acid residues consisting of the "motif". X-ray crystal structure of BR (PDB code: 1C3W) is shown from a view parallel to the membrane. The central part is magnifiedand and the helix C is shown in pink. Three "motif" residues, D85, T89 and D96, are shown in sticks together with the retinal bound to K216 *via* PSB. The corresponding residues in MrHR, T74, S78 and D85 are indicated in the parentheses. (*B*) Comparison of the important residues especially the motifs among the ion pumps.

**FIGURE 3.** Light-induced pH changes by MrHR expressed in *E. coli* cells. The cells were suspended in a 200 mM salt solution without (solid lines) and with (broken lines) 10 μM CCCP.

**FIGURE 4.** Retinal isomer compositions of MrHR in dark and light-adapted states. (*A*) HPLC chromatographs of the retinal isomer extracted from MrHR. (*B*) Ratios of all-*trans* and 13-*cis* retinals determined from the peak areas. The all-*trans* configuration was dominant (> 98%), independent of the dark and light-adapted states.

**FIGURE 5.** Spectroscopic characterization of MrHR. (*A*) Absorption spectral redshift by the $Cl^-$ binding to the unphotolyzed state. The medium (pH 6.5) contained 33 mM $Na_2SO_4$, 0.05% DDM and NaCl (0 - 100 mM). (*B*) Titration with various anions, which were added by sodium salts. The relative absorbance changes at 550 nm were plotted. (*C*) Flash-induced absorbance changes at selected wavelengths. The medium (pH 6.5) contained 0.05% DDM and 100 mM NaCl.

**FIGURE 6.** Characterizations of T74D MrHR. (*A*) Absorption spectra in the unphotolyzed state. The medium (pH 6.5) contained 0.05% DDM and 33 mM $Na_2SO_4$ (solid line) or 500 mM NaCl (broken line). (*B*) Light-induced pH changes by T74D expressed in *E.coli* cells in 200 mM NaCl without and with 10 μM CCCP. (*C*) Flash-induced absorbance changes at selected wavelengths. The medium (pH 6.0) contained 0.05% DDM and 100 mM NaCl.

**TABLE 1**

**Dissociation constants ($K_d$), absorption maxima ($\lambda_{max}$) and their shifts ($\Delta\lambda_{max}$) by the anion bindings**

[a] $K_d$s were determined by fitting analyses using Hill equation with n = 1. The best-fit curves are shown in Fig 5B.

[b] $\lambda_{max}$s were the determined values at the following anion concentrations: $Cl^-$, 0.5 M; $Br^-$, 0.5 M; $I^-$, 0.5 M; $NO_3^-$, 2 M. At these concentrations, the $\lambda_{max}$ shifts were almost saturated.

[c] $\Delta\lambda_{max}$s denote the $\lambda_{max}$ shifts from the anion-free state (506 nm).

| Anions | $K_d$ (mM)[a] | $\lambda_{max}$ (nm)[b] | $\Delta\lambda_{max}$ (nm)[c] |
|---|---|---|---|
| $Cl^-$ | 1.99 ± 0.11 | 537 | 31 |
| $Br^-$ | 0.28 ± 0.08 | 538 | 32 |
| $I^-$ | 2.99 ± 0.21 | 535 | 29 |
| $NO_3^-$ | 171 ± 20.6 | 532 | 26 |

Figure 1

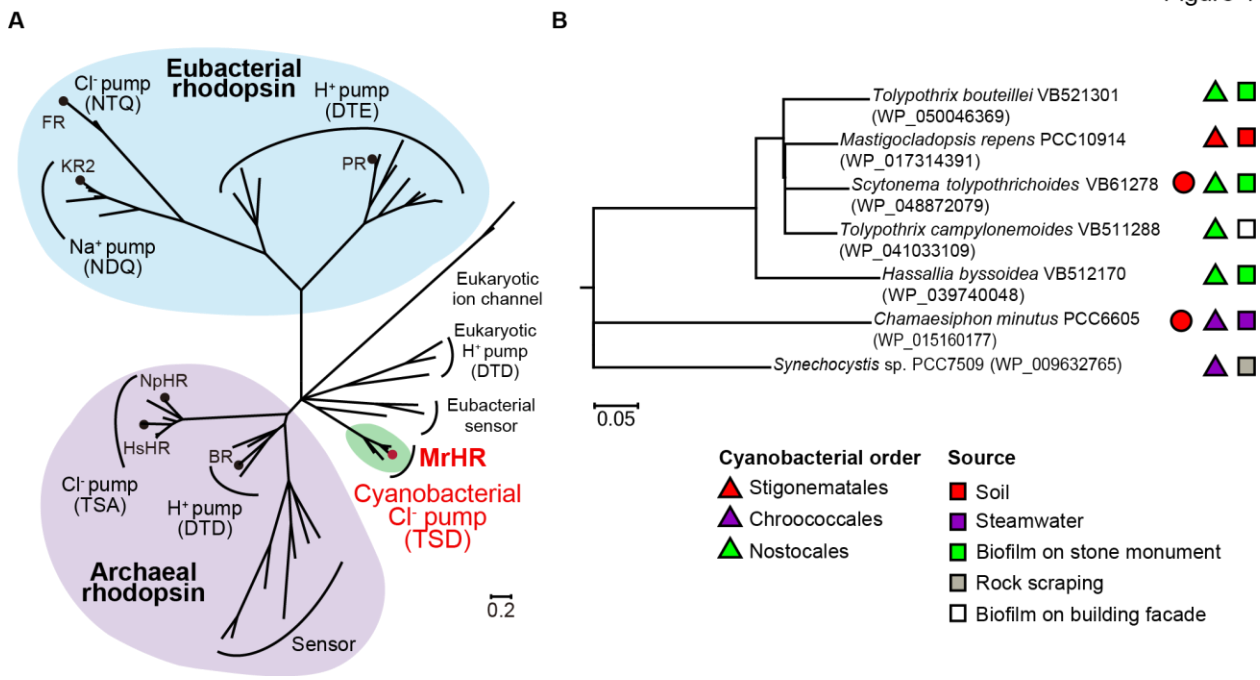
A
Eubacterial rhodopsin
Cl⁻ pump (NTQ)
FR
KR2
Na⁺ pump (NDQ)
H⁺ pump (DTE)
PR
Eukaryotic ion channel
Eukaryotic H⁺ pump (DTD)
Eubacterial sensor
MrHR
Cyanobacterial Cl⁻ pump (TSD)
NpHR
HsHR
BR
Cl⁻ pump (TSA)
H⁺ pump (DTD)
Archaeal rhodopsin
Sensor
0.2
B
Tolypothrix bouteillei VB521301 (WP_050046369)
Mastigocladopsis repens PCC10914 (WP_017314391)
Scytonema tolypothrichoides VB61278 (WP_048872079)
Tolypothrix campylonemoides VB511288 (WP_041033109)
Hassallia byssoidea VB512170 (WP_039740048)
Chamaesiphon minutus PCC6605 (WP_015160177)
Synechocystis sp. PCC7509 (WP_009632765)
0.05
Cyanobacterial order
Stigonematales
Chroococcales
Nostocales
Source
Soil
Steamwater
Biofilm on stone monument
Rock scraping
Biofilm on building facade

Figure 2

A

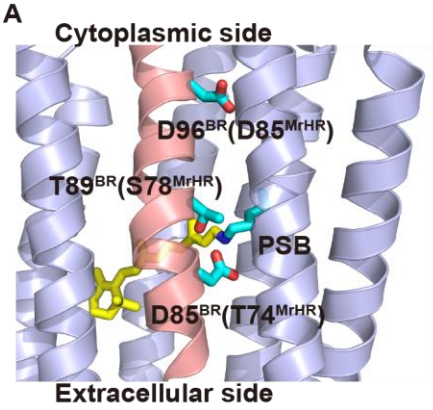


B

| No. in BR | | 82 | **85** | **89** | **96** | 194 | 204 | 212 | 216 |
|---|---|---|---|---|---|---|---|---|---|
| No. in MrHR | | 71 | **74** | **78** | **85** | 182 | 192 | 200 | 204 |
| $H^+$ pump | **BR** | R | **D** | **T** | **D** | E | E | D | K |
| | **PR** | R | **D** | **T** | **E** | L | L | D | K |
| $Na^+$ pump | **KR2** | R | **N** | **D** | **Q** | L | R | D | K |
| $Cl^-$ pump | **FR** | R | **N** | **T** | **Q** | L | R | D | K |
| | **NpHR** | R | **T** | **S** | **A** | E | T | D | K |
| | **MrHR** | R | **T** | **S** | **D** | E | E | D | K |

Figure 3

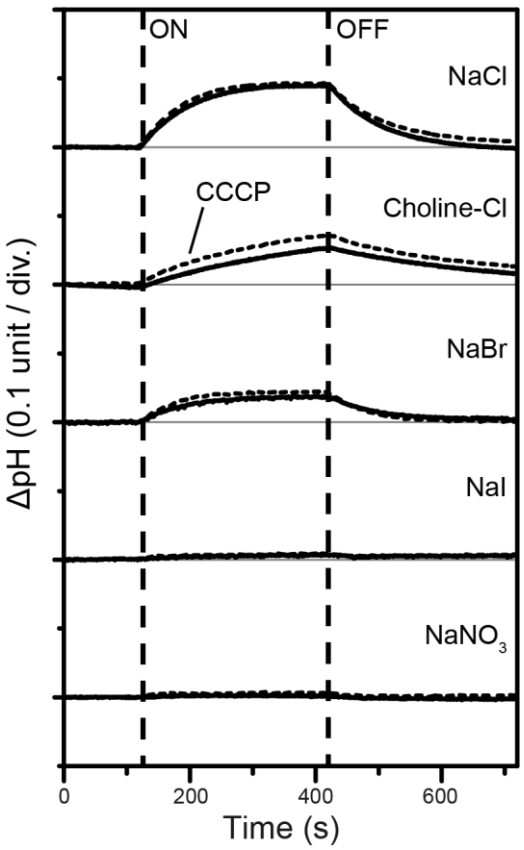
ON
OFF
NaCl
CCCP
Choline-Cl
NaBr
NaI
NaNO3
ΔpH (0.1 unit / div.)
0
200
400
600
Time (s)

Figure 4

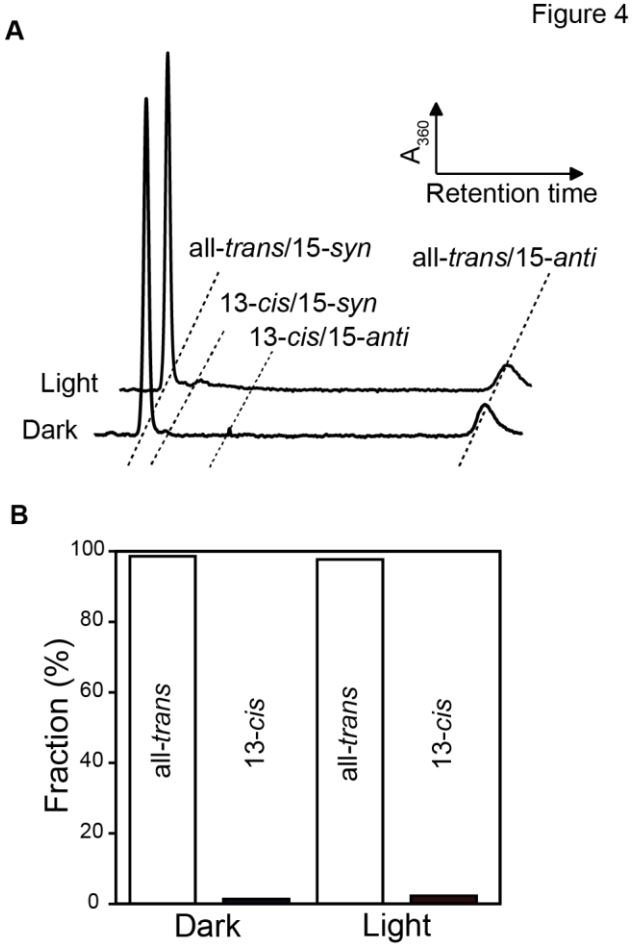
A
$A_{360}$
Retention time
all-*trans*/15-*syn*
all-*trans*/15-*anti*
13-*cis*/15-*syn*
13-*cis*/15-*anti*
Light
Dark
B
Fraction (%)
100
80
60
40
20
0
all-*trans*
13-*cis*
all-*trans*
13-*cis*
Dark
Light

Figure 5

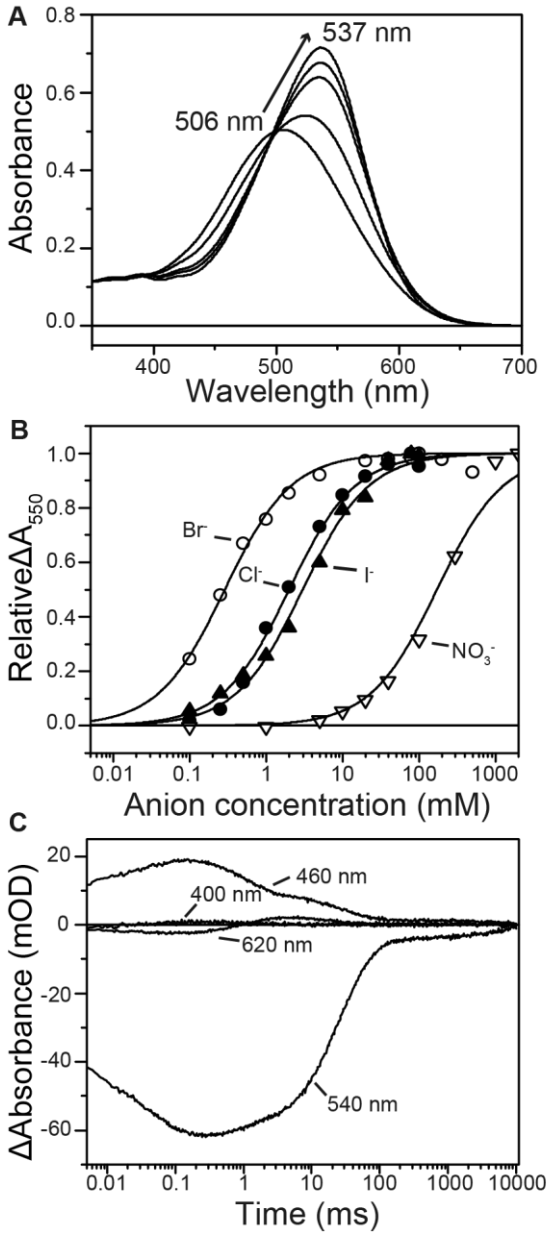
A
537 nm
506 nm
Absorbance
Wavelength (nm)
B
Br-
Cl-
I-
NO3-
RelativeΔA550
Anion concentration (mM)
C
460 nm
400 nm
620 nm
540 nm
ΔAbsorbance (mOD)
Time (ms)

Figure 6

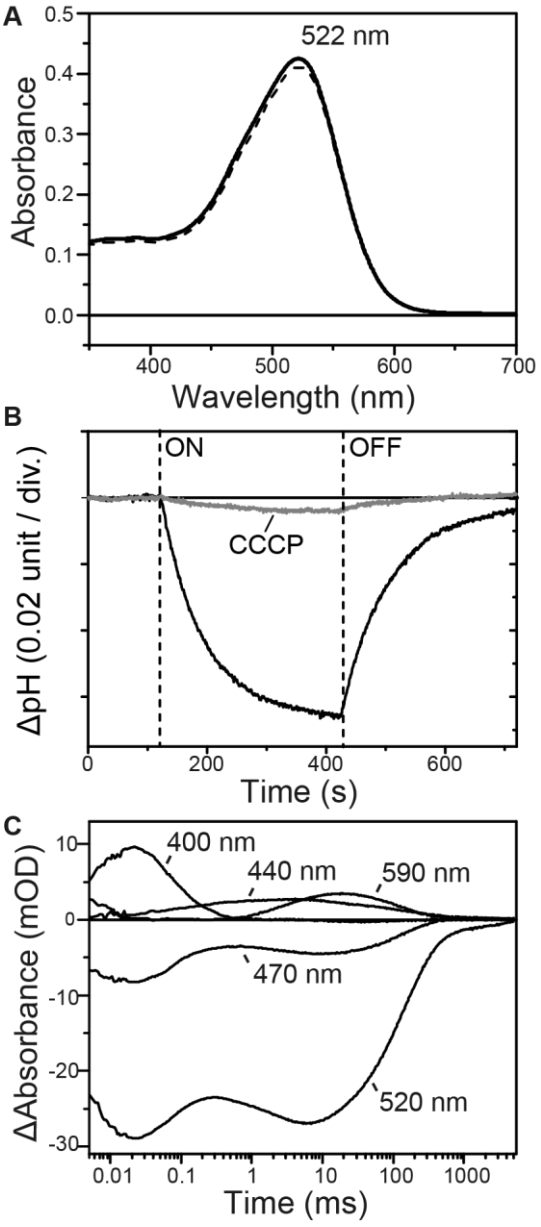
A
522 nm
Absorbance
Wavelength (nm)
B
ON
OFF
CCCP
ΔpH (0.02 unit / div.)
Time (s)
C
400 nm
440 nm
590 nm
470 nm
520 nm
ΔAbsorbance (mOD)
Time (ms)